

# Characterization of bacterial dyes for dye-sensitized solar cells applications

Wan Hasalehah Wan Alli, Nurashikin Suhaili\* and Tay Meng Guan

Faculty of Resource Science and Technology, UNIMAS, 94300 Kota Samarahan, Sarawak, MALAYSIA

\*snurashikin@unimas.my

## Abstract

Bacterial dyes have attracted significant attention as sustainable alternatives to conventional synthetic dyes in dye-sensitized solar cells (DSSCs). Present research has concentrated on a narrow selection of bacterial species, leaving the potential of numerous other pigments largely unexplored. This study aims to characterize pigments extracted from *Chromobacterium violaceum* and *Ralstonia* sp. and to determine their potential as photosensitizers in DSSCs. The pigments were analysed in terms of their spectroscopic and structural properties, determined by Ultraviolet visible and Fourier-Transform Infrared spectroscopy. The DSSCs efficiency of the pigments was also investigated.

Our results showed that the pigments produced by the aforementioned bacteria were identified as violacein and carotenoid. Preliminary investigation into the feasibility of the pigments showed the promising utility of both pigments as photosensitizers for DSSCs. This study provides useful insights into the potential of novel bacterial pigments as photosensitizers for the development of cost-effective and ecologically friendly DSSCs.

**Keywords:** Bacterial pigments, Carotenoid, DSSCs, Photosensitizers, Natural dyes, Violacein.

## Introduction

The exploration of sustainable and environmentally friendly alternatives for energy production is paramount in addressing the growing global energy demands and mitigating the adverse effects of fossil fuels. Dye-sensitized solar cells (DSSCs) have emerged as a promising technology due to their cost-effectiveness, ease of fabrication and potential for high efficiency under diverse lighting conditions. The crucial component of DSSCs is the dye used for sensitization which plays a crucial role in capturing sunlight and converting it into electrical energy.

Traditional synthetic dyes, although effective, often pose environmental and health hazards due to their toxic and non-biodegradable nature. Consequently, there is an increasing interest in identifying and utilizing natural dyes, which can be extracted from plants and pigmented microorganisms, as sustainable alternatives in DSSCs applications.

Concerns have arisen regarding large-scale plant-based pigment extraction due to its impact on the ecosystem, including deforestation and the infringement on local species<sup>12</sup>. On the other hand, bacterial pigments offer a unique and compelling solution to the challenges associated with conventional dyes as well as plant dyes. Bacterial pigments can be produced sustainably through fermentation processes, thus avoiding deforestation and habitat destruction which are otherwise associated with plant pigment extraction. Furthermore, in comparison to plants, bacteria have more rapid growth rate enabling more efficient and quicker pigment production. This has made bacterial pigments a viable option for large-scale DSSCs production. In addition, bacterial dyes are typically non-toxic, biodegradable and can be sourced from renewable resources.

Recent advancements in the use of bacterial pigments as photosensitizers in DSSCs have demonstrated promising results, although the scope of research remains relatively narrow. For instance, Lilwani and co-workers<sup>11</sup> brought to light the potential of carotenoids from *Rhodococcus kroppenstedtii* as photosensitizers in DSSCs. The research demonstrated the capability of carotenoids in absorbing light effectively which indicates its notable conversion efficiency. The use of pigment extracts from *Talaromyces atroroseus* GH2 for developing DSSCs was also reported<sup>28</sup>. A research by Abdul and co-workers<sup>1</sup> explored the enhancement of prodigiosin production by *Serratia nematodiphila* using oil substrate supplementation for potential application in DSSCs. The use of prodigiosin pigment derived from the bacterium *Serratia marcescens* 11E was demonstrated as a sensitizer in DSSCs<sup>8</sup>.

The research demonstrates the promising potential of prodigiosin pigment, which exhibits photoelectric properties that can contribute to the efficiency of the solar cells. Furthermore, the potential of pigments produced by UV-resistant red and yellow psychrotolerant bacteria, isolated from the soils of King George Island, Antarctica, was also reported as photosensitizers in DSSCs<sup>19</sup>. Through analysis of metabolic characteristics and 16S rDNA sequencing, the pigmented bacteria were identified as *Hymenobacter* sp. (red) and *Chryseobacterium* sp. (yellow).

The aforementioned findings indicated that bacterial pigments could be effectively harnessed for DSSCs applications. Despite these advances, there still remains a gap in the comprehensive characterization and application of bacterial pigments for DSSCs. Current research has focused on a limited range of bacterial species, leaving the potential of many other pigments especially by local bacteria

\* Author for Correspondence

unexplored. Moreover, the efficiencies reported for bacterial pigments are relatively low compared to those achieved with plant-based or synthetic dyes, suggesting the need for further optimisation and understanding of these natural photosensitizers.

Therefore, the primary aim of this work was to uncover the potential of pigments produced by locally isolated *Chromobacterium violaceum* and *Ralstonia* sp. for DSSCs applications. The work involved characterizing the extracted pigments using UV-VIS and FTIR spectroscopy to determine their spectroscopic and structural characteristics. Following the characterization studies, the work focused on the evaluation of the pigments as photosensitizers for DSSCs applications. By achieving these objectives, this research seeks to advance the understanding of bacterial dyes in the context of renewable energy applications.

## Material and Methods

**Cultivation of pigmented bacteria:** *Chromobacterium violaceum* and *Ralstonia* sp. were obtained from Environmental and Plant Biotechnology Laboratory, Faculty of Resource Science and Technology, UNIMAS. The bacteria were cultured on Tryptic Soy Agar (TSA) for *C. violaceum* and nutrient agar (Oxoid, UK) for *Ralstonia* sp. Both cultures were incubated at room temperature for 24 hours (*C. violaceum*) and 48 hours (*Ralstonia* sp.).

**Extraction and purification of bacterial pigments:** The *C. violaceum* and *Ralstonia* sp. cultures were scraped and mixed with methanol using a vortex. The suspension was centrifuged at 10000 rpm and at 0 °C for 5 minutes. The resulting supernatant was further concentrated using a rotary evaporator. The extracted pigments were partially purified by mixing them with dichloromethane in a ratio of 1:1. Two layers were formed and the colourless solution was discarded. Then, 1:1 ratio of sodium chloride was added in the dye resulting in double layers whilst the colourless solution was discarded. About 15 g of anhydrous sodium carbonate was added to the solution to remove excess water before the suspension was filtered using a filter paper. The resulting solution was placed in a glass Petri dish and it was left at room temperature until the solvent evaporated. Methanol was added to re-liquefy the sample for further investigation.

**Preparation of titanium dioxide coated ITO glass for DSSCs:** Indium tin oxide (ITO) glass was cleaned in series with propanol, acetone and deionised water for 10 minutes each using an ultrasonic cleaner. The scotch tape was pasted on the conductive side of ITO glass to fix the active area as 3.5 cm<sup>2</sup> (3 cm x 1.5 cm). Titanium dioxide paste was prepared by mixing 1 g of TiO<sub>2</sub> with 2 mL of anatase liquid TiO<sub>2</sub> with 0.8 g of 6000 polyethylene glycol and a few drops of Triton-X 100. The resulting mixture was then mixed well.

The coated glass was then placed in a furnace at 450 °C for 30 minutes, after which it was allowed to cool to room

temperature. Subsequently, the glass was immersed in a solution containing pigment extracts for 24 hours.

**Tri-iodide electrolyte preparation:** The electrolyte was prepared by mixing 8.45 g of 0.5 M potassium iodide and 1.27 g of 0.05 M iodine in 100 ml of polyethylene glycol in a 250 ml conical flask. The mixture was stirred until the mixture was completely dissolved. The resulting electrolyte was then stored in a dark place until it was ready for use.

**DSSCs assembly:** Two glass slides were used to assemble the DSSCs. One glass slide was coated with a smooth layer of TiO<sub>2</sub> using a clean glass rod and then air-dried for one minute. Afterwards, the glass slide was sintered in a furnace at 450 °C for 30 minutes and allowed to cool to room temperature. The TiO<sub>2</sub>-coated slide was then immersed in the extracted dye for 24 hours, protected from light exposure. After dye immersion, the slide was gently washed with ethanol and dried. The other glass slide was prepared as a carbon counter electrode by applying carbon paint, following the same method used for layering the TiO<sub>2</sub>. A drop of iodide electrolyte solution was placed between the positive (TiO<sub>2</sub>-coated) and negative (carbon-coated) electrodes and the two slides were clipped together to form a sandwich-like structure.

**Fabrication of DSSCs:** The fabrication of DSSCs was carried out following a method by Alhamed and co-workers<sup>4</sup> with slight modifications. The setup included a resistor box (DoMore, China), alligator clips, a lamp and a voltmeter (XEOLE, China). The sandwiched DSSCs, resistor box and voltmeter were connected in a parallel circuit, as illustrated in the diagram. The current values were calculated using the formula,  $I=V/R$ . The resistance of the circuit was systematically decreased to obtain the current values and the corresponding voltage values were measured. The current density was then calculated by dividing the current values with the active site area of 1 cm<sup>2</sup>. Graphs of current density (mA/cm<sup>2</sup>) against voltage (mV) were plotted.

The fabrication of the DSSCs was performed by immersing the treated TiO<sub>2</sub> in the target dye overnight, resulting in dye adsorption. Colour changes were observed. The white titanium dioxide turned red, purple and yellow after being immersed in prodigiosin, violacein and carotenoid pigments respectively. Traces of pigments and other constituents were washed off with ethanol and blotted dry to ensure no particles disrupted the electron flow in the circuit. The photoanode, titanium dioxide, was deposited using the doctor blade technique. This method was chosen for its simplicity as it requires only a glass rod to uniformly distribute the photoanode onto the ITO glass.

The efficiency ( $\eta$ ) of DSSCs was calculated by measuring the area under the graph of current density vs voltage using the formula:

$$\eta = \frac{J_{sc} \times V_{oc} \times FF}{P_{in}} \quad (1)$$

The Fill Factor (FF) of the cells was calculated with the formula:

$$FF = \frac{J_{max} \times V_{max}}{J_{sc} \times V_{oc}} \quad (2)$$

The power input was the light illuminated from the white lamp which is 100 mW/cm<sup>2</sup>.

**Ultraviolet visible (UV-Vis) spectrophotometry:** The absorbance rate in the visible light spectrum and the intensity composition of the dye color were determined by measuring the wavelength of light absorbed using a UV-Vis spectrophotometer (Jasco V-630, USA). The dye etching method<sup>22</sup> was employed to dissolve the sample for analysis. This involved rinsing the sample from the glass with methanol and collecting the solution.

The collected solution was then placed into a UV-Vis cuvette for analysis. The pigment was analyzed for maximum absorbance between 400 nm and 650 nm using methanol as a blank. The peaks in the UV-vis results were used to determine the pigment concentration and band gap. The pigment content in the sample was calculated using the following formula:

$$\frac{A \times MW \times DF \times 10^3}{\epsilon \times l} \quad (3)$$

where  $A = A_{max} - A_{700}$ , MW is the molecular weight for the pigments; 343.34 g/mol for violacein<sup>24</sup> and 536.888 g/mol for carotenoid<sup>29</sup>, DF is the dilution factor,  $10^3$  is the factor for conversion from g to mg,  $l$  is the assumed path length of incident light in cm and  $\epsilon$  is molar extinction coefficient which can be calculated using the following formula:

$$\epsilon = \frac{A}{lC} \quad (4)$$

where  $A$  represents the absorbance value of the pigment,  $l$  is the length of cuvette and  $C$  is the molarity of the sample. The samples were dried to obtain the dry weight for the calculation of molarity.

Band gap can be calculated using the following formula:

$$E = \frac{hc}{\lambda} \quad (5)$$

where  $E$  represents photon energy,  $h$  is the plank constant  $6.63 \times 10^{-24}$  Js,  $c$  is the speed constant  $3.0 \times 10^8$  m/s and  $\lambda$  is the corresponding wavelength.

Absorption coefficient determines how far light of a specific wavelength can penetrate into a material before being absorbed. The absorption coefficient of respective wavelength was determined using the following formula:

$$\frac{4\pi k}{\lambda} \quad (6)$$

where  $K$  represents the Boltzman constant  $3.6173324 \times 10^{-5}$  ev and  $\lambda$  stands for the cut-off's wavelength of the dyes.

**Fourier-Transform Infrared (FTIR) analysis:** The pigments were characterized in terms of the structural characteristics by using FTIR (Thermo Scientific/Nicolet I S10, USA). The analysis was performed at a wavelength from 400 to 40000 cm<sup>-1</sup>.

## Results and Discussion

**Optical characteristics of bacterial dyes:** Table 1 outlines the optical characteristics of the bacterial pigments studied in this work. All the three targeted bacterial pigments were found to absorb wavelength within the visible light spectrum, a key characteristic for acting as dye sensitizers in DSSCs<sup>17</sup>. There are two distinct energy levels in electrons namely Lowest Unoccupied Molecular Orbital (LUMO) and Highest Occupied Molecular Orbital (HOMO) levels in bio molecular organic dyes. Upon the illumination, the excited electrons move from lower energy (LUMO) to higher energy (HOMO). The distance between LUMO with HOMO represents the band gap energy<sup>5</sup>. Dye reduction and oxidation potentials are found in the excited state (LUMO) and the ground state (HOMO), according to the electrochemistry calculation.

Correlations of dye band gaps in contributing to DSSCs performance in past reports include anthocyanins with the band gap of 2.46 eV and with 1.67% efficiency<sup>7</sup>. The dye band gap can be credited for determining the redox potential<sup>10</sup>. However, DSSCs efficiency is influenced by multiple factors beyond the band gap as various parameters can also impact its performance. The pigment that had the highest concentration in this study, was carotenoid with the pigment content of  $1.39 \times 10^5$  mgL<sup>-1</sup> cm<sup>-1</sup>.

Our results showed that violacein contained the lowest band gap energy and the highest pigment content compared to other targeted pigments. High pigment content results in more dye molecules available to bind with TiO<sub>2</sub> molecules. This ensures better interaction of both molecules to transport electron.

**Table 1**  
**Optical characteristics of bacterial pigments studied in this work.**

Dyes	Peak absorbance (nm)	Photon energy (eV)	Absorption coefficient, $\alpha$ (km <sup>-1</sup> )	Pigment content (mgL <sup>-1</sup> cm <sup>-1</sup> )	Sample concentration (mol L <sup>-1</sup> )
Carotenoid	420	2.967	2.848	$1.39 \times 10^5$	0.1229
Violacein	570	2.181	1.802	$1.07 \times 10^5$	0.0641

The extracted violacein is able to transfer lower energy electrons to higher energy electron upon the illumination of light faster than the other two pigments due to lower band gap. Figure 2 shows the dependence of absorption coefficient on the wavelength of pigments. The results showed that higher wavelength absorbed by the dye resulted in small band gap leading to better DSSCs efficiency. The lowest photon energy occurred at 570 nm wavelength contributes to small band gap, which is favourable to fasten electron transfer from lower energy to higher energy. The difference between valence band and conduction band is defined as energy band gap, which is used in analysing the performance of DSSCs related to solar energy absorbed.

Light source

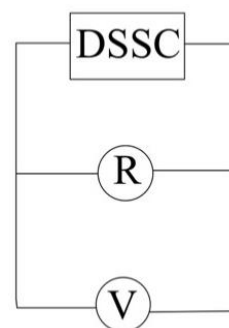


Figure 1: Circuit set up of DSSCs diagram.

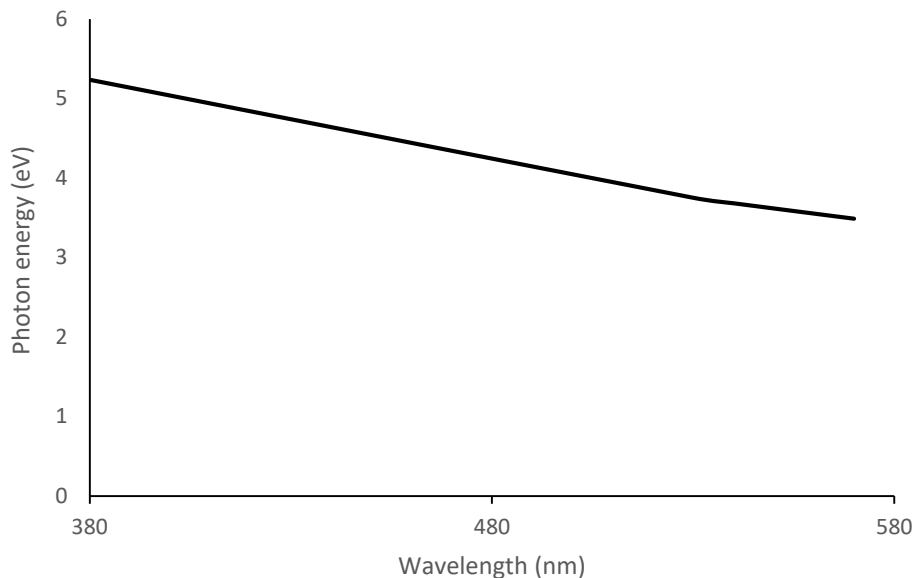


Figure 2: Dependence of absorption coefficient on the wavelength of pigment.

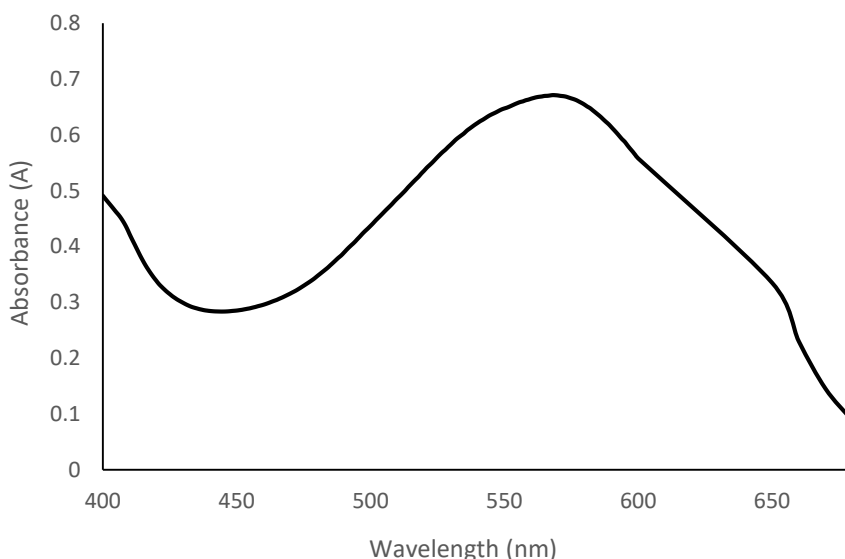
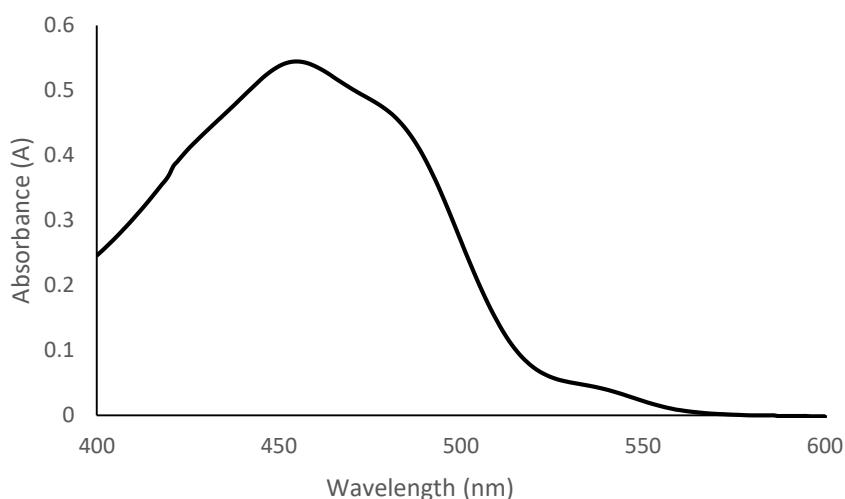
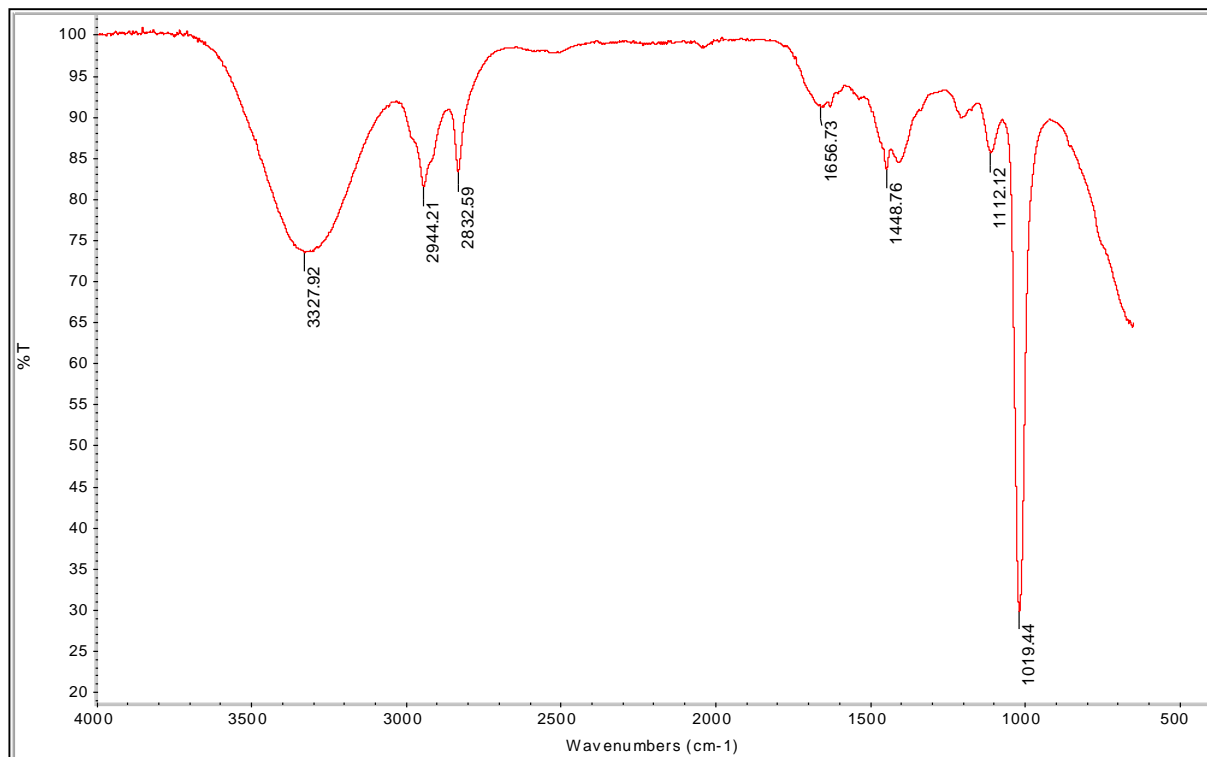


Figure 3: UV-Vis spectrum of the purple pigment.



**Figure 4: UV-Vis spectrum of the yellow pigment.**



**Figure 5: FTIR analysis of the purple pigment.**

**UV-Vis spectrophotometry analysis:** UV-Vis spectrophotometry analysis is a crucial technique that allows characterization of various chemical compounds based on their absorption spectra. Figures 3 and 4 show the UV-Vis spectrum of the purple pigment and yellow pigment respectively. The results showed that the maximum absorbance peak for purple pigment is 570 nm with the absorbance value of 0.669. According to Neshati<sup>18</sup>, the conjugation of C=C in violacein resulted in the absorbance peak ranging from 550 nm to 580 nm. Our results corresponded to the findings reported by Ahmad and co-

workers<sup>2</sup> whereby they reported that the UV-Vis absorbance peak for purple pigment was at 567 nm with the absorbance value of 0.707.

On the other hand, a study reported the maximum absorption violacein extracted from *Janthinobacterium* sp. to be at 757 nm<sup>13</sup>. The presence of chromophores such as alkene and carbonyl groups resulted in the aforementioned UV-Vis absorption range. The carbonyl group absorbs strongly at short UV Vis wavelengths, but as the wavelength increases, the strength diminishes due to the presence of n electrons.

As a result, the alkene groups play an important part in the conjugation effect, where if the more conjugated double bonds are present, the longer will be the absorption wavelength (bathochromic shift)<sup>2</sup>.

The characteristic absorption of carotenoid is between 400 nm and 550 nm<sup>6</sup>. As shown in figure 4, the extracted yellow pigment was found to exhibit broad maximum peak at 450 nm (black line) with the absorbance value of 0.5395. This is in parallel with the findings of some of previous works. For instance, the maximum absorption of pigments from  $\beta$ -carotene akin to zeaxanthin was reported at 456 nm<sup>26</sup>. In another work<sup>16</sup>, the absorption spectrum of the carotenoid pigment by *Paracoccus marcusii* RSPO1 was 460 nm. The presence of chromophore group in carotene is responsible for the measured spectra<sup>19</sup>.

**FTIR analysis:** Some of the parameters that should be considered in the selection of an ideal bio-pigment for DSSCs include available functional groups, chemical (covalent) and physical bonds, number of conjugated double-bonds (n) and length of the organic hydrocarbon structure chain. For strong binding and attachment of dye molecules onto the semiconductor surface, hydrocarbon chains with a lot of hydroxylic (–OH), carboxylic (–COOH) and (=O) radicals are preferred, as the compounds results in lower electron resistance and easier electron injection<sup>2,30</sup>. FTIR analysis gives insights into the functional group possessed by the extracted pigments. Figures 5 and 6 illustrate the FTIR analysis of purple and yellow pigment respectively.

The spectral analysis of FTIR for violacein dissolved in methanol gave values of 3327.92 cm<sup>-1</sup>, 2944.21 cm<sup>-1</sup>, 2832.59 cm<sup>-1</sup>, 1656.73 cm<sup>-1</sup>, 1448.76 cm<sup>-1</sup>, 1112.12 cm<sup>-1</sup> and 1019.44 cm<sup>-1</sup>. The broad spectrum in 3500 – 3300 cm<sup>-1</sup> range centered at 3327.92 resulted from the presence of N–H group on the indole nucleus which is preferred in binding and attachment onto TiO<sub>2</sub> where it facilitates the electron injection in DSSCs. Secondary amides form dimers of cis and trans configuration through hydrogen bonding result in the replacement of the free N–H stretching band. Two peaks stretching at 2944.21 cm<sup>-1</sup> and 2832.59 cm<sup>-1</sup> was contributed by the stretching of C–H of the alkane group.

The peaks at 1656.73 cm<sup>-1</sup> and 1448.76 cm<sup>-1</sup> were obtained from C=O amide groups. The lower frequency band is predominantly N–H in – plane bending (amide II band) and the higher frequency is predominantly C=O (amide I band). This doublet is quite prevalent in amides, where the higher frequency band is primarily C=O (amides I band) and the lower frequency band is primarily N–H in plane bending (amide II band). Since the carbonyl group is conjugated to an aromatic ring, the electrons of both unsaturated groups delocalised, reducing the double bond character of both bonds and lowering the carbonyl frequency from 1718 cm<sup>-1</sup> (normal absorption frequency of carbonyl) to 1656.73 cm<sup>-1</sup>. The resonance is responsible for the lower absorption

frequencies of C=O groups which will be an anchoring group to bind with TiO<sub>2</sub><sup>30</sup>.

Similarly, FTIR results from a report on violacein<sup>3</sup> is in agreement with the results of purple pigment extracted in this work. They described the violacein functional group from FTIR spectra with the stretching of O–H group that might overlap with N–H stretching of secondary amides that corresponded to 3256.53 cm<sup>-1</sup>. Depiction of C=O is similar to this work with the value of 1657.07 cm<sup>-1</sup> and stretching of C=C frequency with the value of 1613.18 cm<sup>-1</sup>. C–O stretching was characterized with the peak at 1223.69 cm<sup>-1</sup>.

Evaluation of the chemical composition of yellow pigment from *Ralstonia* sp. resulted in the transmittance value of 3279.20 cm<sup>-1</sup>, 1639.59 cm<sup>-1</sup>, 1404.17 cm<sup>-1</sup>, 1014.38 cm<sup>-1</sup>, 590.33 cm<sup>-1</sup> and 555.39 cm<sup>-1</sup> as shown in figure 6. Based on a report by Supriyanto and co-workers<sup>25</sup>, wide range of values from 3300 cm<sup>-1</sup> – 2800 cm<sup>-1</sup> resulted from the vibration of OH in the carboxylic acid in the carotenoid structure which is crucial in TiO<sub>2</sub> binding with the bacterial pigment. The resilient vibration occurs due to the compression of the band. Ordenes and co-workers<sup>19</sup> reported the carotenoid FTIR spectra of yellow pigment from Antarctic bacteria with the spectra frequency of 3300 cm<sup>-1</sup> which corresponded to the absorption band for the vibration of the OH group. This is in agreement with the results of this work where the spectra frequency was found to be 3279.20 cm<sup>-1</sup>.

A feature of carbonyl group (C=O) was observed from the signal at 1639.59 cm<sup>-1</sup>. This could be due to the oxidation of zeaxanthin, lycopene or lutein. Oxidation happens when oxygen is incorporated into either of the C=C double bonds or when the OH group in the chemical structure of the carotenoid is oxidized<sup>31</sup>. The peak at 1404.17 cm<sup>-1</sup> resulted in the bending C–H of the alkane and 1014.38 cm<sup>-1</sup> due to bending of C=C with disubstitution. The pattern of this result shows similarities in carotenoid<sup>21</sup>. The FTIR results and UV spectra from the previous works suggest that the yellow pigment from *Ralstonia* sp. falls under the carotenoid family (zeaxanthin, lutein or mixture of both).

### Photo electrical properties of DSSCs

**Efficiency of DSSCs developed using violacein:** The performance of DSSCs was evaluated by connecting the circuit to a multimeter and a resistor in series exposing it to white light to obtain the efficiency curve graph which describes the relationship between voltage and density current. From the efficiency graph, power was determined by multiplying the current with the voltage. Figures 7 and 8 show the efficiency of DSSCs developed using violacein and carotenoid respectively.

From the efficiency graphs, two parameters namely open voltage (VOC) and short circuit (ISC) can be determined. The X-intercept is VOC whilst the Y-intercept is ISC. Therefore, VOC from the prodigiosin efficiency graph was

318 mV whilst the ISC is  $0.012 \text{ mA/cm}^2$ . VOC obtained from the carotenoid and violacein efficiency graphs was 303 mV and 240 mV respectively. Furthermore, the short circuit current (ISC) retrieved from the carotenoid and violacein efficiency graphs was 0.035 and  $0.012 \text{ mA/cm}^2$  respectively. Bacterial carotenoid from the report by Ordenes and co-workers<sup>19</sup> reported VOC of 548.79 mV paired with ISC of  $0.13 \text{ mA/cm}^2$ , higher than the findings of carotenoid from this research.

There is a high possibility that the dye molecules from this research did not adhere well to  $\text{TiO}_2$  film halting the clear

pathway for electrons transport. Upon the illumination of light, pigment dyes molecule becomes excited by injecting electrons to conduction band of  $\text{TiO}_2$  nanoparticle films. The redox electrolyte provides recirculation of electrons and at the same time creating a path for electron transport<sup>20</sup>. Therefore, the DSSCs device converts sunlight energy to electrical energy when illuminated with light and current and voltage data can be obtained from the external circuit. As shown in figures 7 and 8, DSSCS employing bacterial pigments exhibited expected behaviour of solar cells attest by expected current-voltage curve.

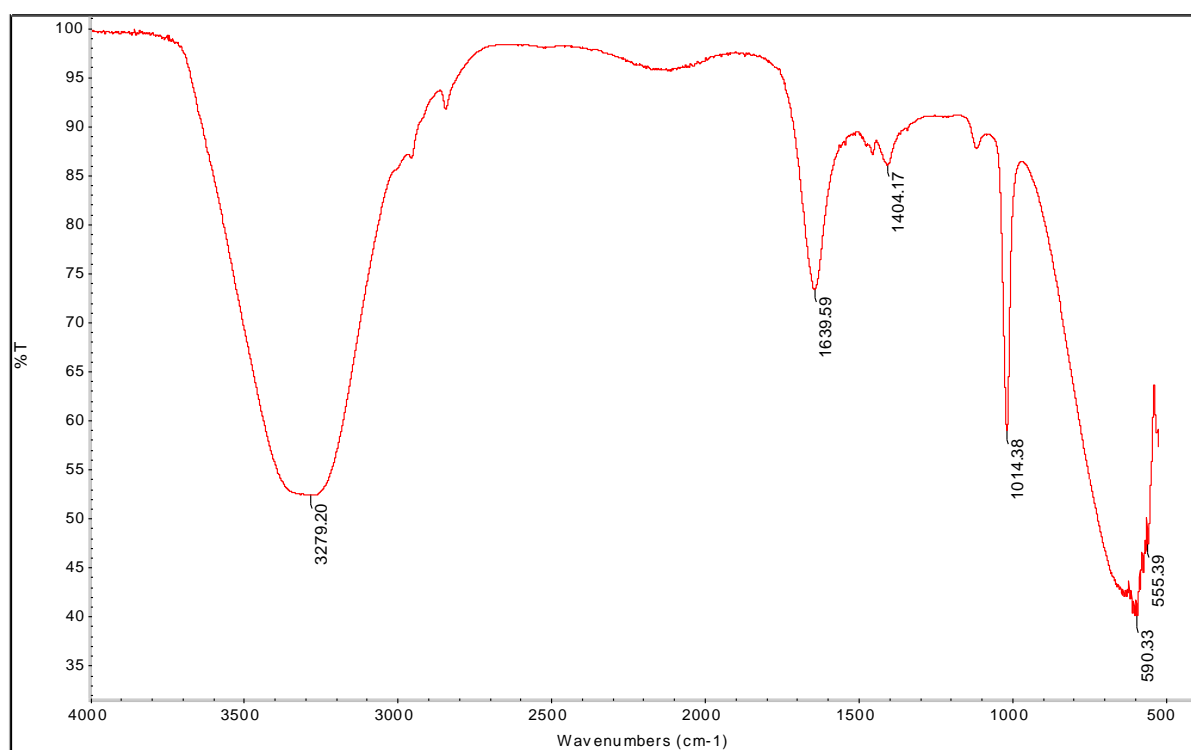


Figure 6: FTIR analysis of yellow pigment

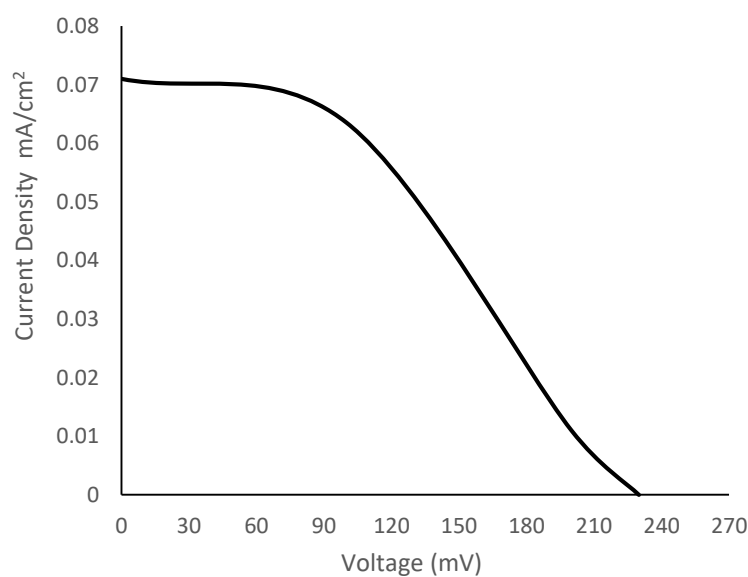


Figure 7: Efficiency of DSSCs developed using violacein.

No photo-voltage responses were observed under darkness due to minimal density of charge carriers in the valence band and the presence of the indication of diode character in sensitized  $\text{TiO}_2$  and electrolyte interface named Schottky barrier. In the presence of light, the dynamic response in the intermittent status implicates the occurrence of processes such as photo-regeneration, recombination and diffusion of electrons<sup>27</sup>.

Figures 9 and 10 show the relationship between power and voltage of DSSCs developed using carotenoid and violacein. The power curves show the maximum power points, which are the optimal working points of the cells. The maximum power for carotenoid and violacein was 3.89 mW and 6.36

mW respectively. It can be observed that DSSCs that used violacein generated higher power than carotenoid.

The maximum power achieved by DSSCs using all the three pigments in this work was found to be lower than that reported in the literature. For instance, DSSCs developed using red dragon fruit pigment produced maximum power of 35 mW<sup>15</sup>. The development of DSSCs using melanin isolated from *S. filodesensis* with the pigment concentration of 6500  $\mu\text{g}/\text{ml}$  was reported where the maximum power produced was 3910 mW<sup>23</sup>. The variation of maximum power can be associated with the source of the pigments as well as the pigment concentration used in developing DSSCs.

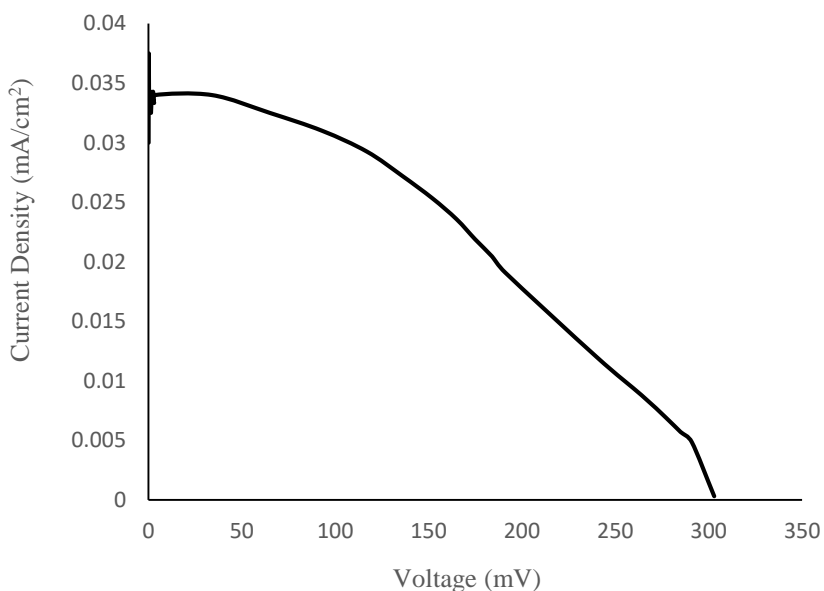


**Figure 8: Efficiency of DSSCs developed using carotenoid.**

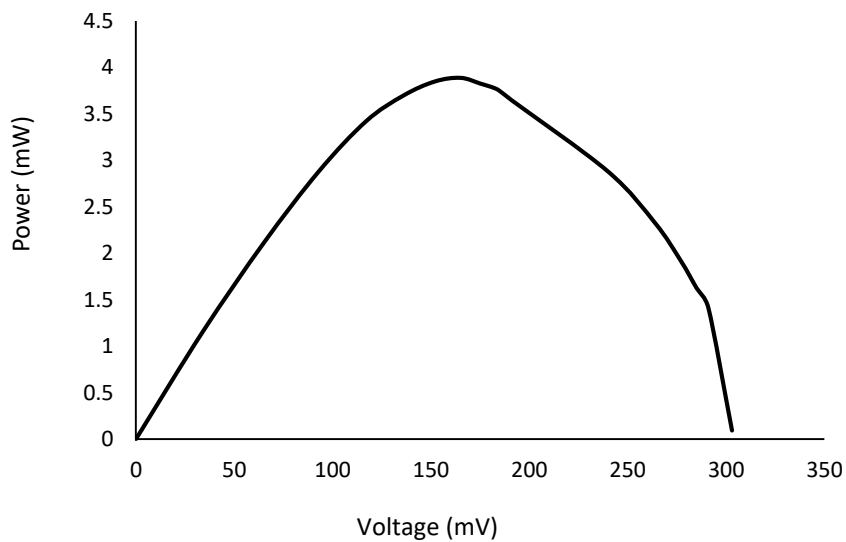


**Figure 9: Power versus voltage characteristic curve for DSSCs using carotenoid pigment as photosensitizer.**

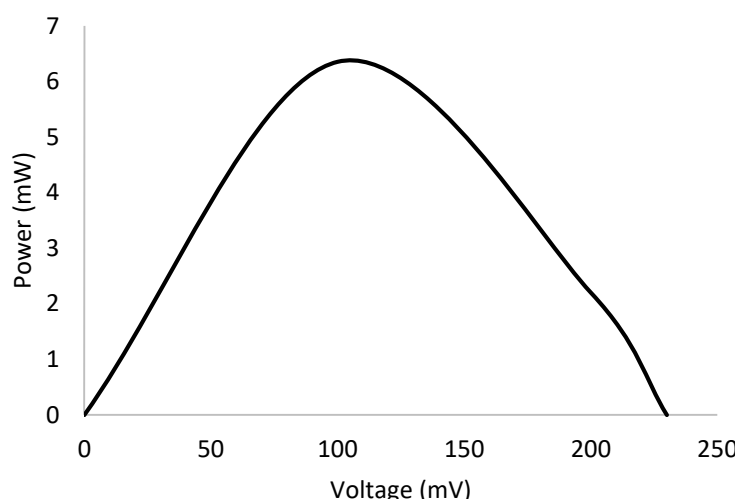


**Figure 10: Power versus voltage characteristic curve for DSSCs using violacein pigment as photosensitizer.**

**Table 2**  
**Photoelectrical properties of extracted bacterial pigments.**

Pigments	Source of pigment	Short circuit current, $J_{sc}$ (mA/cm <sup>2</sup> )	Open circuit voltage, $V_{oc}$ (mV)	Fill Factor, FF (%)	Efficiency, $\eta$ (%)
Carotenoid	<i>Ralstonia</i> sp.	0.035	313	0.3488	0.0382
Violacein	<i>C. Violaceum</i>	0.071	318	0.5802	0.0806

Table 2 shows the short circuit current ( $J_{sc}$ ), open circuit voltage ( $V_{oc}$ ), fill factor (FF) and efficiency percentage of DSSCs developed using carotenoid and violacein. Violacein has the highest FF amongst the two pigments as 0.58%. The FF represents the measure of closeness in a solar cell and it acts as an ideal source. Solar cell fill factor is a metric that measures the efficiency of a solar PV module. The solar cell fill factor has an impact on the solar panel because it influences the efficiency of the panel by affecting the cell series values. It also has an influence on solar panel energy efficiency by altering the shunt resistances and diode losses.

When the shunt resistance of a solar cell is increased, the series resistance lowers, resulting in a larger FF. Meanwhile, larger FF in a solar cell means that the cell is more efficient, resulting in a higher output power that matches the theoretical maximum<sup>9</sup>. However, even though with the highest fill factor value, prodigiosin produces the lowest power input compared to the other two pigments due to lower short circuit current produced. This may be caused by high resistance in the circuit limiting the current production.

The results from this work showed that violacein pigment had the highest efficiency of 0.0806%. This implies that the violacein pigment in the DSSCs converted 0.0806% of the solar energy into electrical power. In a work by Ordenes-Aenishanslins et al<sup>19</sup>, only *Chryseobacterium* sp. and *Hymenobacter* sp. were reported as sources of carotenoid. The efficiency of carotenoid in this work (0.0382%) is comparable to that extracted from *Chryseobacterium* sp. and

*Hymenobacter* sp. which were 0.0323% and 0.0332% respectively<sup>19</sup>. The efficiency of DSSCs developed using violacein in this research (0.0806%) was lower than the efficiency of DSSCs using a pigment produced by *Janthinobacterium* sp. UV13, which was 0.23%<sup>13</sup>. The low efficiency in this work may be caused by improper interaction of bacterial pigments with  $TiO_2$  which may decrease the optimal electron transport in the circuit. The instability of electrolyte also affects the efficiency of electron reload within the cell.

The concentration of bacterial pigments present in the sample facilitates the electron transportation by increasing the chances of dye molecules adhering onto the  $TiO_2$  nanoparticles. This can be supported by the results shown in table 2 where violacein with the highest pigment concentration exhibited the highest efficiency among all the pigments. There are a few factors that can explain the behaviour of the efficiency of DSSCs in this work. Violacein has the lowest band gap energy as calculated in table 1 which insinuates that low energy is required for the pigment to excite the dye molecules which are essentials in improving electron transportation. Electron transportation is crucial in DSSCs efficiency as the movement of the electron along the circuit generates current.

## Conclusion

In conclusion, this work characterizes pigments extracted from *Ralstonia* sp. and *C. violaceum* known as carotenoid and violacein respectively as photosensitizers in DSSCs.

Our results suggest that these pigments hold potential for DSSCs applications. This is based on their ability to absorb photons across a broad range of 400 – 600 nm. The DSSCs efficiency for carotenoid and violacein was 0.038% and 0.081% respectively.

This study provides valuable insights into the development of cost-effective and ecologically friendly DSSCs using novel bacterial pigments as photosensitizers. Future work should explore the integration of the bacterial pigments into large scale DSSCs prototypes as well as the evaluation of their stability and long-term performance.

## References

1. Abdul Manas N.H., Chong L.Y., Tesfamariam Y.M., Zulkharnain A., Mahmud H., Abang Mahmud D.S., Mohamad Fuzy S.F.Z. and Wan Azelee N.I., Effects of oil substrate supplementation on production of prodigiosin by *Serratia nematodiphila* for dye-sensitized solar cell, *J. Biotechnol.*, **317**, 16–26 (2020)
2. Ahmad W.A., Ahmad W.Y.W., Zakaria Z.A. and Yusof N.Z., Application of Bacterial Pigments as Colorant: The Malaysian Perspective, Springer Science & Business Media (2011)
3. Ahmad W.A., Ahmad W.Y.W., Zakaria Z.A. and Yusof N.Z., Isolation of pigment-producing bacteria and characterization of the extracted pigments, In Application of Bacterial Pigments as Colorant, Springer, Berlin, Heidelberg, 25–44 (2012)
4. Alhamed M., Issa A.S. and Doubal A.W., Studying of natural dyes properties as photo-sensitizer for dye sensitized solar cells (DSSCs), *J. Electron Devices*, **16(11)**, 1370-1383 (2012)
5. Calogero G., Yum J.H., Sinopoli A., Di Marco G., Grätzel M. and Nazeeruddin M.K., Anthocyanins and betalains as light-harvesting pigments for dye-sensitized solar cells, *Sol. Energy*, **86(5)**, 1563–1575 (2012)
6. Dieser M., Greenwood M. and Foreman C.M., Carotenoid pigmentation in Antarctic heterotrophic bacteria as a strategy to withstand environmental stresses, *Arct. Antarct. Alp. Research*, **42(4)**, 396–405 (2010)
7. Hao S., Wu P., Huang Y. and Lin J., Natural dyes as photosensitizers for dye-sensitized solar cell, *Sol. Energy*, **80**, 209–214 (2006)
8. Hernández-Velasco P. et al, Photoelectric evaluation of dye-sensitized solar cells based on prodigiosin pigment derived from *Serratia marcescens* 11E, *Dyes Pigms.*, **177**, 108278 (2020)
9. Jao M.H., Liao H.C. and Su W.F., Achieving a high fill factor for organic solar cells, *J. Mater. Chem. A*, **4(16)**, 5784–5801 (2016)
10. Kim C.W., Suh S.P., Choi M.J., Kang Y.S. and Kang Y.S., Fabrication of  $\text{SrTiO}_3$ – $\text{TiO}_2$  heterojunction photoanode with enlarged pore diameter for dye-sensitized solar cells, *J. Mater. Chem. A*, **1 (38)**, 11820–11827 (2013)
11. Lilwani S., Khan M.A.R.P. and Vernekar M., Exploring carotenoid from *Rhodococcus kroppenstedtii* as a photosensitizer in a dye sensitised solar cell, *Def. Life Sc. J.*, **8(2)**, 111-115 (2023)
12. López-Cruz R., Sandoval-Contreras T.D.J. and Iñiguez-Moreno M., Plant pigments: Classification, extraction and challenge of their application in the food industry, *Food Bioprocess Tech.*, **16**, 2725-2741 (2023)
13. Marizcurrena J.J., Castro-Sowinski S. and Cerdá M.F., Improving the performance of dye-sensitized solar cells using nanoparticles and a dye produced by an Antarctic bacterium, *Environ. Sustain.*, **4**, 711–721 (2021)
14. Mohan V.M., Shimomura M. and Murakami K., Improvement in performances of dye-sensitized solar cell with  $\text{SiO}_2$ -coated  $\text{TiO}_2$  photoelectrode, *J. Nanosci. Nanotechnol.*, **12(1)**, 433-438 (2012)
15. Motlan and Siregar N., The efficiency of natural dyes-based dye sensitised solar cells, *J. Phy. Sc.*, **32(1)**, 57-68 (2021)
16. Naik R. and Gupte S., Characterization of pigment produced by high carotenoid yielding bacteria *Paracoccus marcusii* RSPO1 and evaluation of its anti-diabetic, anti-microbial and antioxidant properties, *Nat. Prod. Res.*, **38(6)**, 968–977 (2024)
17. Narayan M.R., Review: Dye sensitized solar cells based on natural photosensitizers, *Renew. Sustain. Energy Rev.*, **16 (1)**, 208–215 (2012)
18. Neshati, A., Extraction and characterization of purple pigment from chromobacterium violaceum grown in agricultural wastes, Universiti Teknologi Malaysia (2010)
19. Órdenes-Aenishanslins N., Anziani-Ostuni G., Vargas-Reyes M., Alarcón J., Tello A. and Pérez-Donoso J.M., Pigments from UV-resistant Antarctic bacteria as photosensitizers in dye sensitized solar cells, *J. Photochem. Photobiol. B.*, **162**, 707–714 (2016)
20. O'Regan B. and Grätzel M., A low-cost, high-efficiency solar cell based on dye-sensitized colloidal  $\text{TiO}_2$  films, *Nature*, **353(6346)**, 737–740 (1991)
21. Saha S.K., Rahman M.A., Sarkar M.R.H., Shahjahan M. and Khan M.K.R., Effect of Co doping on structural, optical, electrical and thermal properties of nanostructured ZnO thin films, *J. Semicond.*, **36(3)**, 033004 (2015)
22. Shahzad N., Pugliese D., Lamberti A., Sacco A., Virga A., Gazia R. and Pirri C.F., Monitoring the dye impregnation time of nanostructured photoanodes for dye sensitized solar cells, *J. Phys.*, Conf. Ser. (2013)
23. Silva C., Santos A., Salazar R., Lamilla C., Pavez B., Meza P., Hunter R. and Barrientos L., Evaluation of dye sensitized solar cells based on a pigment obtained from Antarctic *Streptomyces fildesensis*, *Sol. Energy*, **181**, 379-385 (2019)
24. Subramaniam S., Ravi V. and Sivasubramanian A., Synergistic antimicrobial profiling of violacein with commercial antibiotics against pathogenic microorganisms, *Pharm. Biol.*, **52(1)**, 86–90 (2014)
25. Supriyanto A., Nurosyid F. and Ahliha A.H., Carotenoid pigment as sensitizers for applications of dye-sensitized solar cell (DSSC), IOP Conf. Ser.: Mater. Sci. Eng., **432**, 012060 (2018)

26. Tátraaljai D., Major L., Földes E. and Pukanszky B., Study of the effect of natural antioxidants in polyethylene: Performance of  $\beta$ -carotene, *Polym. Degrad. Stab.*, **102**, 33-40 (2014)

27. Tello A., Gómez H., Muñoz E., Riveros G., Pereyra C.J., Dalchiele E.A. and Marotti R.E., Electrodeposition of nanostructured ZnO thin films from dimethylsulfoxide solution: Effect of temperatures on the morphological and optical properties, *J. Electrochem. Soc.*, **159**(12), D750 (2012)

28. Tropea A., Spadaro D., Trocino S., Giuffrida D., Ruiz-Sánchez J.P., Montañez J., Morales-Oyervides L., Dufossé L., Mondello L. and Calogero G., Development of dye-sensitized solar cells using pigment extracts produced by *Talaromyces atroroseus* GH2, *Photochem. Photobiol. Sci.*, **23**, 941–955 (2024)

29. Van Breeman R.B., Innovations in carotenoid analysis using LC/MS, *Anal. Chem.*, **68** (9–11), 299–304 (1996)

30. Wang Z.S., Yamaguchi T., Sugihara H. and Arakawa H., Significant efficiency improvement of the black dye-sensitized solar cell through protonation of TiO<sub>2</sub> films, *Langmuir*, **21**(10), 4272–4276 (2005)

31. Zheng Y.T., Toyofuku M., Nomura N. and Shigeto S., Correlation of carotenoid accumulation with aggregation and biofilm development in *Rhodococcus* sp. SD-74, *Anal. Chem.*, **85**(15), 7295–7301 (2013).

(Received 18<sup>th</sup> August 2024, accepted 19<sup>th</sup> October 2024)